

See discussions, stats, and author profiles for this publication at: <https://www.researchgate.net/publication/227180367>

# Block Liposome and Nanotube Formation is a General Phenomenon of Two-Component Membranes Containing Multivalent Lipids

ARTICLE *in* SOFT MATTER · SEPTEMBER 2011

Impact Factor: 4.03 · DOI: 10.1039/C1SM05481C · Source: PubMed

---

CITATIONS

3

READS

61

## 6 AUTHORS, INCLUDING:



Kai Ewert

University of California, Santa Barbara

76 PUBLICATIONS 1,568 CITATIONS

[SEE PROFILE](#)



Bridget Carragher

New York Structural Biology Center

171 PUBLICATIONS 6,047 CITATIONS

[SEE PROFILE](#)



# NIH Public Access

## Author Manuscript

*Soft Matter.* Author manuscript; available in PMC 2012 June 13.

Published in final edited form as:  
*Soft Matter.* 2011 January 1; 7(18): 8363–8369. doi:10.1039/C1SM05481C.

## Block Liposome and Nanotube Formation is a General Phenomenon of Two-Component Membranes Containing Multivalent Lipids

Alexandra Zidovska<sup>1,2,\*</sup>, Kai K. Ewert<sup>1</sup>, Joel Quispe<sup>3</sup>, Bridget Carragher<sup>3</sup>, Clinton S. Potter<sup>3</sup>, and Cyrus R. Safinya<sup>1,\*</sup>

<sup>1</sup>Materials, Physics, and Molecular, Cellular and Developmental Biology Departments, University of California at Santa Barbara, Santa Barbara, CA 93106

<sup>2</sup>Dept. of Systems Biology, Harvard Medical School, Boston, MA 02115 and School of Engineering and Applied Sciences/Dept. of Physics, Harvard University, Cambridge, MA 02138

<sup>3</sup>National Resource for Automated Molecular Microscopy, Department of Cell Biology, The Scripps Research Institute, 10550 North Torrey Pines Road, La Jolla, CA 92037

### Abstract

We report a study on the formation of block liposomes (BLs) and nanotubes from membranes comprised of mixtures of membrane curvature-stabilizing multivalent cationic lipids MVL3(3+) and MVL5(5+) with neutral 1,2-dioleoyl-*sn*-glycero-3-phosphatidylcholine (DOPC). In conjunction with prior work on MVLBG2(16+), our experiments suggest that BL and nanotube formation is a general phenomenon in membranes containing multivalent lipids, thus enhancing the relevance of BLs for applications such as gene/drug storage and delivery or templating.

### Keywords

block liposomes; lipid bilayer; curvature-stabilizing lipids; membrane curvature

### Introduction

Recently, we reported the formation of a new class of chain-melted (liquid) liposomes, termed block liposomes (BLs)<sup>1</sup>, in mixtures of the highly charged curvature-stabilizing multivalent lipid MVLBG2<sup>2</sup> (headgroup charge +16 e) and the neutral lipid 1,2-dioleoyl-*sn*-glycero-3-phosphatidylcholine (DOPC) at  $\Phi_{MVLBG2}=0.1$  in water with no added salt. Pure DOPC, in contrast, does not form BLs. Hallmarks of BLs are linked liposome shapes such as vesicles and micelles. In a BL, liposome shapes comprised of lipid bilayers such as spheres, pears, and tubes, but also micelles comprised of a lipid monolayer (in particular cylindrical micelles, also called nanorods in this work), are connected into one object. A detailed characterization of BLs by cryogenic transmission electron microscopy (cryo-TEM) led to a model for their formation that suggests an interplay of membrane undulations and concentration fluctuations of the two lipid components. These lead to the phase separation of MVLBG2 and DOPC, with MVLBG2 grouping into the regions of high membrane

\*alexandra\_zidovska@hms.harvard.edu, safinya@mrl.ucsb.edu.

**Supporting Information Available:** Description of materials and experimental methods; chemical structures of DOPC, DOTAP, MVL3, MVL5, and MVLBG2; differential-interference-contrast (DIC) optical micrographs of MVL3/DOPC and MVL5/DOPC mixtures; additional cryo-TEM images of block liposomes formed by MVL3 and MVL5.

curvature, such as nanotubes and nanorods, and DOPC concentrating in the locally flat (zero curvature) regions, such as bilayer spheres of large radius frequently attached to the end of a nanotube/nanorod<sup>1</sup>.

Further investigations exposing BLs to varied pH and salt conditions identified both the high charge as well as the high membrane curvature provided by MVLBG2 (due to the large headgroup) as prerequisites for BL-formation<sup>3</sup>. In those experiments the extent of electrostatic screening was controlled by the salt content in the solution. Changes in pH altered the protonation of MVLBG2, thus changing its charge as well as the size of its headgroup, leading to various liposomal shape transitions dependent on the extent of alterations. Understanding the shape evolution of BLs under different environmental conditions is highly relevant to both applications and basic biological science: BLs are promising candidates for lipid-based gene and drug delivery<sup>4-7</sup> and templating of other nanostructures such as wires and needles<sup>8-10</sup>, and many biological processes such as endocytosis, endoplasmatic reticulum-associated vesiculation, vesicle recycling and signaling take advantage of liposome shape changes<sup>11-16</sup>.

In this report we present a cryo-TEM study on the formation of block liposomes from membranes comprised of mixtures of the membrane curvature-stabilizing multivalent lipids, MVL3<sup>17</sup>, MVL5<sup>18</sup> and MVLBG2<sup>2,19</sup> with charges of +3, +5, and +16 e, respectively, and DOPC. The chemical structures of these lipids can be found in the Supporting Information (Fig. S1). The work presented in this report focuses on cationic lipids because of their importance for nonviral delivery of nucleic acids such as DNA and siRNA. Both MVL3/DOPC and MVL5/DOPC lipid mixtures in water exhibit a regime of BL-formation with pronounced nanotube formation at  $\Phi_{MVL3} = 0.1$  and  $0.3$  and  $\Phi_{MVL5} = 0.1$ . Our experiments thus suggest that the formation of BLs is a general phenomenon in membranes containing multivalent charged lipids, thus highlighting the relevance of BLs for applications such as gene/drug storage and delivery or templating.

Interestingly, new and unique features were found in the BLs formed by MVL3 and MVL5. Lipid mixtures of MVL3 and DOPC form more nanotubes and fewer nanorods, and the nanotubes often exhibit a pearl-like feature, where a nanotube widens into a “bubble” that narrows again to its original radius. MVL3-containing nanotubes also show branching as well as a reduced stiffness compared to the previously studied MVLBG2/DOPC nanotubes. Lipid mixtures of MVL5 and DOPC show a pronounced bundling of the nanotubes. Another key feature of this system is the formation of “spikes”, shorter nanorods budding off from a nanotube, representing a further step of curvature-driven phase separation. In this case, the nanotube is considered a region of lower curvature with respect to the nanorod, a region of extremely high curvature. This is quite remarkable, as the nanotube already possesses a fairly high membrane curvature.

## Materials and Methods

### Materials

DOPC and DOTAP were purchased from Avanti Polar Lipids. MVL3, MVL5 and MVLBG2 were synthesized as described<sup>2,17-19</sup>.

### Lipid Solutions

Lipid stock solutions were prepared in chloroform/methanol (9:1, v/v). Lipid solutions were combined at the desired ratio of lipids and dried, first by a stream of nitrogen and subsequently in a vacuum for 8 to 12 hours. To the residue, high resistivity (18.2 MΩcm) water was added and the mixture incubated at 37 °C for at least 12 hours to give a final concentration of 10 mg/mL. The lipid solutions were stored at 4 °C until use. The lipids

remained in their chain-melted liquid state due to their unsaturated lipid tails. This was confirmed by wide angle X-ray scattering experiments (data not shown).

### Optical Microscopy

A Nikon Diaphot 300 inverted microscope equipped for epifluorescence and DIC and a SensiCam<sup>QE</sup> High Speed digital camera were used.

### Cryo-TEM

The specimens were preserved in a layer of vitreous ice suspended over a holey carbon substrate. The holey carbon films consist of a thin layer of pure carbon fenestrated by 2  $\mu\text{m}$  holes spaced 4  $\mu\text{m}$  apart and suspended over 400 mesh copper grids<sup>20</sup>. The grids were cleaned prior to vitrification with a Solarus plasma cleaner (Gatan Inc.) using a 25% O<sub>2</sub>, 75% Ar mixture. The concentration of the sample solution was typically 5–10 mg/mL. Samples were vitrified by plunge freezing into liquid ethane using a Vitrobot (FEI Co.). Microscopy was carried out using a Tecnai F20 (FEI Co.) TEM at 120 keV with magnifications ranging from 29,000–280,000. Images were acquired at an underfocus of ~2.5  $\mu\text{m}$  to a slow scan CCD camera (TVIPS GmbH) using the Leginon software system<sup>21</sup>.

## Results and Discussion

BLs form in a very narrow composition interval around  $\Phi_{\text{MVLBG2}}=0.1$  in the MVLBG2/DOPC system. Considering this and comparing headgroup geometries and charge, we first screened MVL3/DOPC and MVL5/DOPC mixtures of  $\Phi_{\text{MVL}}=0.1$ –0.5 with differential interference contrast (DIC) microscopy. We then investigated the samples with cryo-TEM. We found micrometer-scale tubular vesicles and BLs for  $\Phi_{\text{MVL}}=0.1$  (see Fig. S2 and S3 in Supporting Information), and both of these mixtures were found to also form nanoscale BLs and nanotubes when investigated with cryo-TEM. In addition, cryo-TEM revealed BL and nanotube formation for the MVL3/DOPC system at  $\Phi_{\text{MVL3}}=0.3$ . No BLs were found for  $\Phi_{\text{MVL}} > 0.3$ .

Fig. 1 shows cryo-TEM images of BLs formed by a mixture of MVL3 and DOPC in water ( $\Phi_{\text{MVL3}}=0.1$ ). In contrast to MVLBG2-containing BLs, where nanotubes and nanorods (cylindrical micelles) are very rigid with a persistence length of several micrometers, MVL3-containing nanotubes are very soft and bend easily. The white solid arrows point to the loci of highest bending. It is noteworthy that there is no preferred orientation of these nanotubes, confirming that the nanotubes are not induced by any flow effects during the sample preparation. Instead, this lipid mixture inherently forms nanotubes. The reduced stiffness of the nanotubes can be explained by the reduced charge of the lipid bilayer. MVL3 only has a charge of +3 e, whereas MVLBG2 has a charge of +16 e. Thus, the electrostatic contribution to the bending modulus  $K$  is strongly reduced<sup>22</sup>.

Further characteristic features of the MVL3/DOPC lipid mixture in water ( $\Phi_{\text{MVL3}}=0.1$ ) are displayed in Fig. 2. Fig. 2 A shows the presence of nanorods (highlighted by white solid arrows). Although present, nanorods are not as abundant as they were in the MVLBG2/DOPC lipid mixture ( $\Phi_{\text{MVLBG2}}=0.1$ ). This observation is consistent with the lower propensity of MVL3 to form micelles due to its smaller headgroup: although MVL3 has a conical molecular shape, the aspect ratio of this molecule is not as extreme as that of MVLBG2. Another key feature of the MVL3/DOPC system is branching of the nanotubes, as seen in Fig. 2 A (highlighted by a white dashed arrow).

The distribution of the diameters of MVL3-containing nanotubes is quite broad as demonstrated in Fig. 2 B. Fig. 2 C provides a schematic drawing of a BL consisting of a sphere and a nanorod as well as an illustration of the molecular organization (in the regions

framed by rectangles) of the multivalent lipid (shown in green) and the neutral lipid (shown in white) as previously suggested for the MVLBG2/DOPC system. Note the high concentration of the charged lipid in the nanorod, where it stabilizes the high curvature.

Fig. 3 A depicts one of the unique hallmarks of the MVL3/DOPC lipid mixture in water ( $\Phi_{MVL3}=0.1$ )—the pearling instability. A pearling instability has previously been described in micrometer-scale tubular vesicles<sup>23</sup> and was attributed to the increased tension in the lipid bilayer<sup>24</sup>. We hypothesize that lipid demixing in the nanotubes leads to a phase separation between charged MVL3 (localized mostly in the nanotubes) and neutral DOPC (localized mostly in the “bubbles”). In fact, the lipid demixing might be initialized by increased membrane tension due to the electrostatic repulsion among MVL3 molecules and their curvature stabilization efforts. In addition, the relatively low stiffness of the MVL3-containing membranes reduces the elastic energy cost of the structures resulting from pearling. Fig. 3 B shows a schematic drawing of a sphere-tube-sphere BL with illustrations of the suggested molecular organization in the nanotube and the tube-sphere transition regions. The transition from nanotube to a vesicle is highly reminiscent of the pearling instability described above. Similar features as described above for the MVL3/DOPC lipid mixture at  $\Phi_{MVL3}=0.1$  were also found for  $\Phi_{MVL3}=0.3$ .

Screening of the phase behavior of MVL5/DOPC lipid mixtures in water showed BL and nanotube formation at  $\Phi_{MVL5}=0.1$ . As clearly visible in Fig. 4, this lipid mixture forms an abundance of long nanotubes and BLs. The length of the nanotubes can be well over 10  $\mu\text{m}$ . The size of the spherical vesicular parts varies widely from tens to hundreds of micrometers. An expanded low magnification cryo-TEM image displaying a larger area of the sample can be found in the Supporting Information (Fig. S4).

The MVL5/DOPC lipid mixture ( $\Phi_{MVL5}=0.1$ ) also exhibits unique features not found in other BL-forming systems. Fig. 5 gives an overview of the key features observed in this system. Standard examples of BLs can be seen in Fig. 5 A (sphere–rod) and Fig. 5 F (sphere–tube). In addition, bundling of nanotubes is abundant in this system. Interestingly, the nanotubes in a bundle frequently cross each other and thus exchange their position in the bundle as shown in Fig. 5 A and B (areas highlighted by white dotted circles) or loop around each other as demonstrated in the example in Fig. 5 C (highlighted by white dotted circle). Finally, a novel feature that we term “spike” can be observed in Fig. 5 D and E (highlighted by white dotted arrows). These spikes are a remarkable feature fully consistent with the concept of BLs. It is a nanorod (cylindrical micelle) budding off perpendicularly from the nanotube side (rather than from the nanotube tip as observed previously<sup>1</sup>). Formation of this feature corresponds to a further curvature-induced phase separation within a nanotube, which itself is already a high-curvature object. In the spikes, the pentavalent MVL5 (essential for stabilizing the high curvature of nanotubes) continues to seek regions of even higher curvature, which can only be achieved by nanorod formation. The kinetics of this system have to be radically different from those of the MVLBG2/DOPC/water system, where the phase separation forming nanorods from nanotubes exclusively occurred at the tips of nanotubes. In contrast, the MVL5/DOPC/water system can nucleate a nanorod at any point along the whole length of a nanotube.

As mentioned earlier, nanotube crossings and loops leading to complicated tubular entanglements are abundant in the MVL5/DOPC system. This is surprising considering the relatively high charge of the lipid bilayer, which should result in an electrostatic repulsive force. Fig. 6 A and B present numerous further examples of such entanglements (highlighted by white dotted circles). White solid arrows point to nanorods and a white dotted arrow to a spike, a feature introduced above. Due to the intermediate headgroup size of MVL5 (larger than MVL3, but smaller than MVLBG2), its propensity to form micelles is also intermediate

and a fair number of lipid nanorods was found. Unfortunately, the presence of a vast number of long nanotubes (similarly to MVL3/DOPC lipid mixture) prevented us from quantifying the number of nanorods because they get harder to discern along their complete length, resulting in possible multiple counts of the same nanorod.

The large extent of nanotube bundling is further illustrated by Fig. 7, which is a superimposition of several high magnification cryo-TEM images (allowing us to review a larger sample area). A further expansion of this collage can be found in the Supporting Information (Fig. S5). The bundle shown in Fig. 7 consists of  $\approx 20$  nanotubes, which are in a surprising proximity considering their large positive charge. A possible explanation for such a tight bundling might be that the entanglements described above mechanically hold the bundle together at several locations along the bundle length. Another explanation might be a favorable surface interaction between the tubules based, for example, on surface charge fluctuations.

Investigation of mixtures of monovalent DOTAP and DOPC in water failed to produce evidence of nanotube or block liposome formation. DOTAP carries a charge of +1 e (cf. Figure S1 in the Supporting Information) and its molecular shape can be described as cylindrical rather than conical ( $C_0 \approx 0$ ). Therefore, the propensity to form micelles is very low. This suggests that formation of BLs and nanotubes requires a certain minimal head group size of the lipid or, in other words, a propensity for micelle formation and thus the ability to stabilize high membrane curvature in addition to charge.

A remarkable aspect of the observed BLs is the presence of regions with negative Gaussian curvature (saddle splay-type surfaces with  $C_1 C_2 < 0$ , where  $C_1$  and  $C_2$  are the membrane principal curvatures) in membranes containing lipids with such large headgroups. Located, e.g., at the transition regions between tubes/rods and vesicles and at nanotube branching points, regions with  $C_1 C_2 < 0$  are a defining feature of BLs: without them, the constituting membrane shapes of a BL would form separate liposomes. Yet this combination of negative Gaussian curvature in structures formed from lipids that induce positive spontaneous curvature due to their large headgroup size ( $C_0 > 0$ ) is unprecedented.

The elastic energy of a lipid bilayer per unit area can be described by Helfrich's relation<sup>25</sup>

$$\frac{F}{A} = \frac{\kappa}{2} (C - C_0)^2 + \kappa_G C_1 C_2 \quad (1)$$

where  $\kappa$  and  $\kappa_G$  are the membrane bending and the Gaussian elastic moduli, respectively,  $C = C_1 + C_2$ , and  $C_0 = 2/R_0$  with the spontaneous radius  $R_0$ . Accordingly, surfaces with negative Gaussian curvature are energetically favored if the Gaussian modulus is positive ( $\kappa_G > 0$ ). The Gaussian modulus is related to  $C_0$  as

$$\kappa_{G,Bilayer} = 2\kappa_{G,Monolayer} - 4\delta C_0 \kappa_{Monolayer} \quad (2)$$

where  $\delta$  is the membrane thickness and  $\kappa_{G,Bilayer/Monolayer}$  are the Gaussian moduli of lipid bilayer and monolayer, respectively. Negative values of  $C_0$  thus increase  $\kappa_{G,Bilayer}$ , favoring the formation of saddle splay surfaces<sup>26</sup>. This is reflected in the fact that lipid systems forming cubic phases (where  $C_1 C_2 < 0$ ) typically also exhibit an inverted hexagonal phase (where  $C < 0$  and  $C_1 C_2 = 0$ ). In contrast, multivalent charged lipids have a conical molecular shape, giving rise to  $C_0 > 0$  and driving the formation of nanotubes and nanorods. It is thus remarkable that nanotubes and nanorods do not detach from spherical vesicles and/or each other, and the reason for this remains unclear. Possibly, an interaction between the multivalent and neutral lipid is essential for BL formation, because BLs do not form when the membranes contain only multivalent lipid. In addition, the electrostatic interaction plays

a key role in BL formation<sup>3</sup> and, therefore, needs to be considered in future theories. A theory of block liposome formation must also be able to predict the characteristic feature of BLs that a single object exhibits length scales varying by as much as two orders of magnitude (e.g., a diblock sphere–rod liposome may exhibit radii of curvature of < 10 nm (diameter of rod) and > 1000 nm (diameter of the spherical component)).

In a recent self-consistent field theory Greenall and Gompper have indeed found that mixtures of amphiphiles with different molecular shapes may form equilibrium block liposome phases<sup>27</sup>. Their starting point is amphiphiles, which separately form lamellar structures and spherical micelles similar to what is found in the mixtures which produce block liposomes: DOPC forms lamellar phases and small curvature vesicles while the highly cone shaped multivalent lipids form micelles<sup>1,28,29</sup>. Their theory shows that the presence of curvature forming amphiphiles in mixtures may lead to curvature induced lateral phase separation of amphiphiles and microphase separation of shapes leading to an equilibrium phase where vesicles connected by thread-like micelles exist at equilibrium in a narrow range of concentrations of the curvature forming amphiphile. This is precisely the hypothesis put forward in the original paper introducing the discovery of block liposomes<sup>1</sup>. The equilibrium structure described by Greenall and Gompper corresponds to a triblock (sphere-rod-sphere) liposome.

We caution that the Greenall-Gompper theory does not take into account electrostatics explicitly (i.e. the amphiphiles are charge neutral), which we know to be important. Thus, the way it fits into our experimental system is as follows. The shape of a lipid depends on the relative size of the headgroup area versus the tail area. There are two components to the headgroup size: steric and that due to charge (i.e. the Debye length<sup>3</sup>). The current theory considers the limit where the steric size alone makes the entire contribution and the headgroup is large enough to make a strong curvature generating lipid. In the experiments described here and earlier<sup>1,3,28</sup> we have found that the added contribution of the charge to the “effective” headgroup size is needed to produce block liposomes. Thus, the theory may be applicable to the experimental system in that it effectively takes into account electrostatics by considering amphiphiles with large enough steric headgroups. The Greenall-Gompper model is an important starting point for a revised model where the charge of the curvature generating amphiphile and the counter-ions are explicitly taken into account.

## Conclusions

In conclusions, our cryo-TEM studies have shown that mixtures of the multivalent cationic lipids MVL3 and MVL5 with neutral DOPC readily form nanotubes and block liposomes. In combination with studies of monovalent DOTAP, where no nanotubes or block liposomes were found, and previous investigations of the phase behavior of hexadecavalent MVLBG2, our data suggests that the formation of nanotubes and block liposomes is an inherent property of charged membranes formed by lipids with a propensity to form micelles, i.e., conical molecular shape ( $C_0 > 0$ ). This is of fundamental importance for the understanding of the shape evolution of liposome systems. The results described in this report should motivate future theories of block liposome formation in multicomponent charged membranes comprised of two lipid components with vastly varying shapes. We emphasize that future models, which may be based on the Greenall-Gompper theory, must incorporate the charged nature of the membrane, which experiments show to be an essential feature of block liposomes<sup>3</sup>. These new theories are required to understand BLs and might allow predicting nanotube formation in other, yet unstudied systems. The present study was motivated mainly by gene therapy and therefore focused on cationic lipids. However, we are aware of an example of brain derived, anionic curvature-generating lipids causing a

spontaneous formation of lipid tubules<sup>30</sup>, which would expand our finding to anionic membranes as well.

## Supplementary Material

Refer to Web version on PubMed Central for supplementary material.

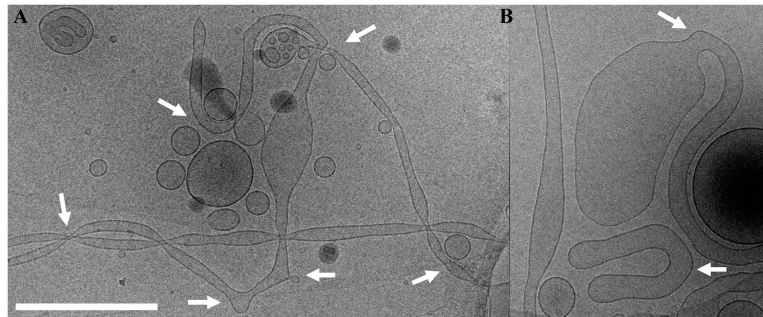
## Acknowledgments

We acknowledge support by NIH grant GM-59288, DOE BES DE-FG02-06ER46314 (lipid phase behavior), and NSF DMR-0803103. AZ is a Damon Runyon Fellow supported by the Damon Runyon Cancer Research Foundation (DRG 2040-10). The cryogenic transmission electron microscopy research was performed at the National Resource for Automated Molecular Microscopy, which is supported by the U. S. NIH National Center for Research Resources P41 program (RR17573). CRS acknowledges useful discussions with KAIST Faculty where he has a WCU (World Class University) Visiting Professor of Physics appointment supported by the National Research Foundation of Korea funded by the Ministry of Education, Science and Technology No. R33-2008-000-10163-0.

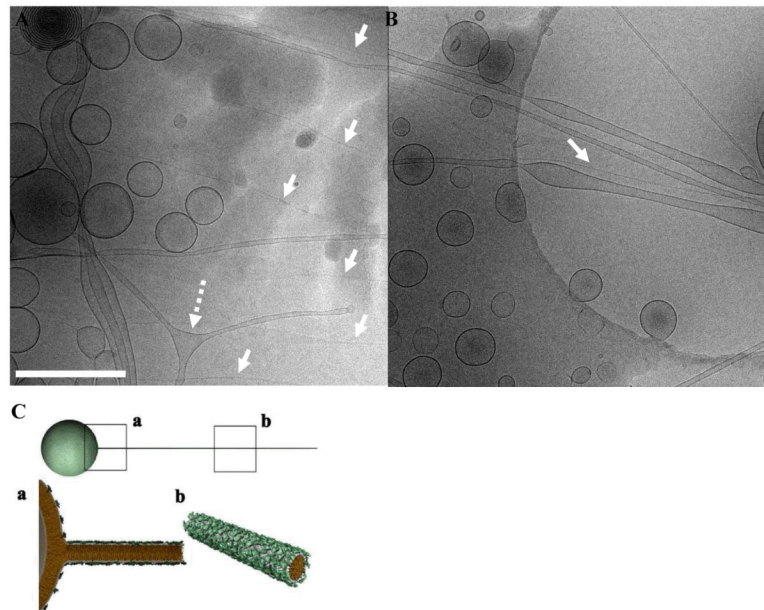
## References

1. Zidovska A, Ewert KK, Quispe J, Carragher B, Potter CS, Safinya CR. Block Liposomes from Curvature-Stabilizing Lipids: Connected Nanotubes, -rods and -spheres. *Langmuir*. 2009; 25:2979–2985. [PubMed: 18834165]
2. Ewert KK, Evans HM, Zidovska A, Bouxsein NF, Ahmad A, Safinya CR. A columnar phase of dendritic lipid-based cationic liposome-DNA complexes for gene delivery: Hexagonally ordered cylindrical micelles embedded in a DNA honeycomb lattice. *J. Am. Chem. Soc.* 2006; 128:3998–4006. [PubMed: 16551108]
3. Zidovska A, Ewert KK, Quispe J, Carragher B, Potter CS, Safinya CR. The effect of salt and pH on block liposomes studied by cryogenic transmission electron microscopy. *Biochim. Biophys. Acta.* 2009; 1788:1869–1876. [PubMed: 19559003]
4. Ewert K, Slack NL, Ahmad A, Evans HM, Lin AJ, Samuel CE, Safinya CR. Cationic lipid-DNA complexes for gene therapy: Understanding the relationship between complex structure and gene delivery pathways at the molecular level. *Curr. Med. Chem.* 2004; 11:133–149. [PubMed: 14754413]
5. Ewert KK, Ahmad A, Evans HM, Safinya CR. Cationic lipid-DNA complexes for nonviral gene therapy: relating supramolecular structures to cellular pathways. *Expert Opin. Biol. Ther.* 2005; 5:33–53. [PubMed: 15709908]
6. Huang, L.; Hung, M-C.; Wagner, E. *Non-Viral Vectors for Gene Therapy*. Elsevier; San Diego: 2005.
7. Mahato, RI.; Kim, SW.; Francis, T. a., editors. *Pharmaceutical Perspectives of Nucleic Acid-Based Therapeutics*. London and New York: 2002.
8. Singh A, Wong EM, Schnur JM. Toward the rational control of nanoscale structures using chiral self-assembly: Diacetylenic phosphocholines. *Langmuir*. 2003; 19:1888–1898.
9. Schnur JM. Lipid Tubules - a Paradigm for Molecularly Engineered Structures. *Science*. 1993; 262:1669–1676. [PubMed: 17781785]
10. Shimizu T, Masuda M, Minamikawa H. Supramolecular nanotube architectures based on amphiphilic molecules. *Chem. Rev.* 2005; 105:1401–1443. [PubMed: 15826016]
11. Alberts, B. *Molecular Biology of The Cell*. Garland Science; New York: 2002.
12. Gallop JL, Butler PJG, McMahon HT. Endophilin and CtBP/BARS are not acyl transferases in endocytosis or Golgi fission. *Nature*. 2005; 438:675–678. [PubMed: 16319893]
13. Gallop, JL.; McMahon, HT. BAR domains and membrane curvature: bringing your curves to the BAR. *Rafts and Traffic; Lipids*; 2005. p. 223-231.
14. Hinshaw JE, Schmid SL. Dynamin Self-Assembles into Rings Suggesting a Mechanism for Coated Vesicle Budding. *Nature*. 1995; 374:190–192. [PubMed: 7877694]

15. Roux A, Cuvelier D, Nassoy P, Prost J, Bassereau P, Goud B. Role of curvature and phase transition in lipid sorting and fission of membrane tubules. *EMBO J.* 2005; 24:1537–1545. [PubMed: 15791208]
16. Qi SY, Groves JT, Chakraborty AK. Synaptic pattern formation during cellular recognition. *Proc. Natl. Acad. Sci. U.S.A.* 2001; 98:6548–6553. [PubMed: 11371622]
17. Ahmad A, Evans HM, Ewert K, George CX, Samuel CE, Safinya CR. New multivalent cationic lipids reveal bell curve for transfection efficiency versus membrane charge density: lipid-DNA complexes for gene delivery. *J. Gen. Med.* 2005; 7:739–748.
18. Ewert K, Ahmad A, Evans HM, Schmidt HW, Safinya CR. Efficient synthesis and cell-transfection properties of a new multivalent cationic lipid for nonviral gene delivery. *J. Med. Chem.* 2002; 45:5023–5029. [PubMed: 12408712]
19. Ewert KK, Evans HM, Bouxsein NF, Safinya CR. Dendritic cationic lipids with highly charged headgroups for efficient gene delivery. *Bioconjugate Chem.* 2006; 17:877–888.
20. Quispe J, Damiano J, Mick SE, Nackashi DP, Fellmann D, Ajero TG, Carragher B, Potter CS. An improved holey carbon film for cryo-electron microscopy. *Microsc. Microanal.* 2007; 13:365–371. [PubMed: 17900388]
21. Suloway C, Pulokas J, Fellmann D, Cheng A, Guerra F, Quispe J, Stagg S, Potter CS, Carragher B. Automated molecular microscopy: The new Leginon system. *J. Struct. Biol.* 2005; 151:41–60. [PubMed: 15890530]
22. Winterhalter M, Helfrich W. Effect of Surface-Charge on the Curvature Elasticity of Membranes. *J. Phys. Chem.* 1988; 92:6865–6867.
23. Barziv R, Moses E. Instability and Pearlting States Produced in Tubular Membranes by Competition of Curvature and Tension. *Phys. Rev. Lett.* 1994; 73:1392–1395. [PubMed: 10056781]
24. Goldstein RE, Nelson P, Powers T, Seifert U. Front propagation in the pearlting instability of tubular vesicles. *J. Phys. II.* 1996; 6:767–796.
25. Helfrich W. Elastic Properties of Lipid Bilayers - Theory and Possible Experiments. *Z. Naturforsch., C: Biosci.* 1973; C 28:693–703.
26. Porte G. Lamellar phases and disordered phases of fluid bilayer membranes. *J. Phys.: Condens. Matter.* 1992; 4:8649–8670.
27. Greenall MJ, Gompper G. Bilayers Connected by Threadlike Micelles in Amphiphilic Mixtures: A Self-Consistent Field Theory Study. *Langmuir.* 2011; 27:3416–3423. [PubMed: 21381728]
28. Zidovska, A.; Ewert, KK.; Quispe, J.; Carragher, B.; Potter, CS.; Safinya, CR. Methods in Enzymology Liposomes. 2009. Block Liposomes: Vesicles of Charged Lipids with Distinctly Shaped Nanoscale Sphere-, Pear-, Tube-, or Rod-Segments; p. 111-128.Pt G
29. Zidovska A, Evans HM, Ewert KK, Quispe J, Carragher B, Potter CS, Safinya CR. Liquid Crystalline Phases of Dendritic Lipid-DNA Self-Assemblies: Lamellar, Hexagonal, and DNA Bundles. *J. Phys. Chem. B.* 2009; 113:3694–3703. [PubMed: 19673065]
30. Akiyoshi K, Itaya A, Nomura SM, Ono N, Yoshikawa K. Induction of neuron-like tubes and liposome networks by cooperative effect of gangliosides and phospholipids. *FEBS Lett.* 2003; 534:33–38. [PubMed: 12527358]

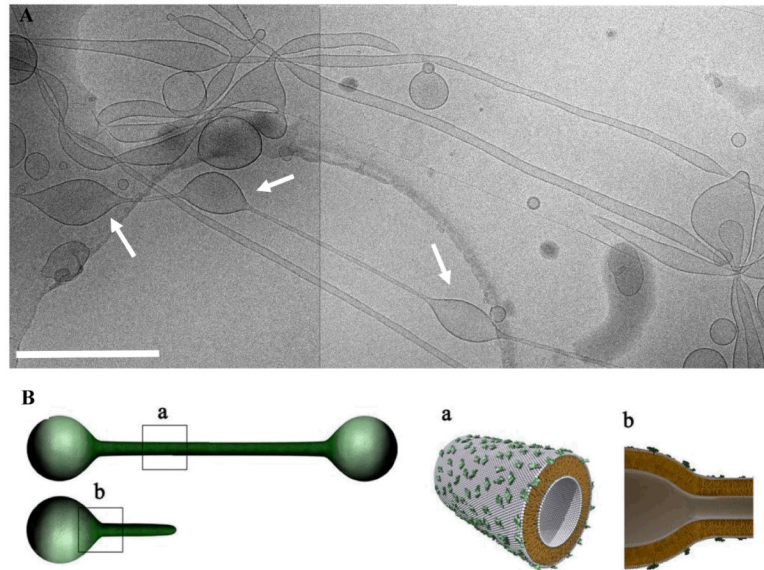
**Figure 1.**

Cryo-TEM images of MVL3/DOPC BLs ( $\Phi_{MVL3}=0.1$ ). Both micrographs clearly show extensive bending of the flexible MVL3-containing nanotubes (white arrows point toward some of the regions where nanotubes are bent). Note the diversity in spatial orientation of the tubes, which confirms that the nanotubes are not formed by flow effects during sample preparation. Scale bar, 500 nm.



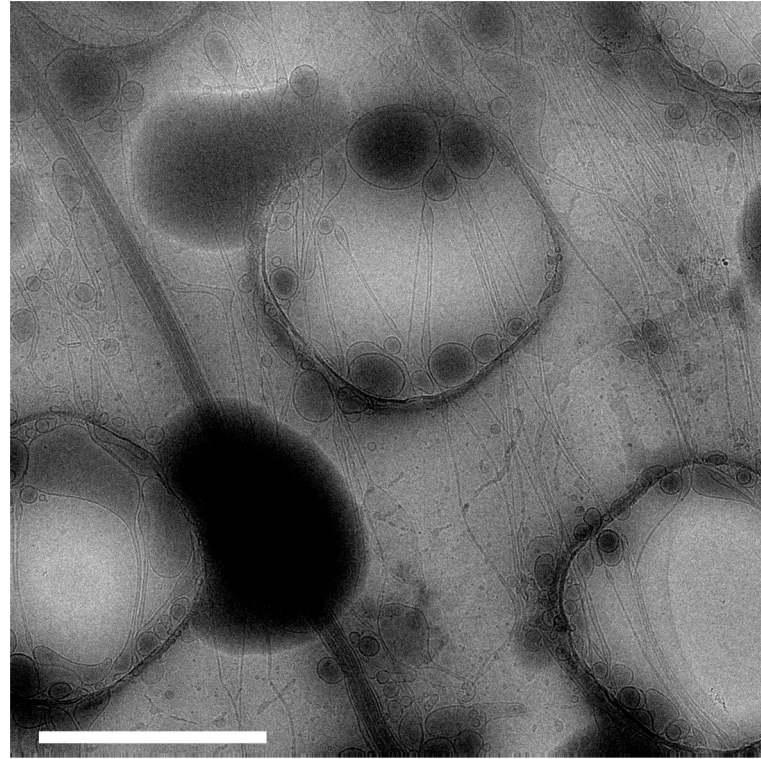
**Figure 2.**

Cryo-TEM images of MVL3/DOPC BLs ( $\Phi_{MVL3}=0.1$ ). (A) A dotted white arrow points to an example of a branched nanotube. White solid arrows point to the nanorods in the sample. (B) A group of nanotubes of different diameter, illustrating the broad distribution of radii of MVL3-containing nanotubes. The white solid arrow points to a nanorod. (C) A schematic drawing of a BL consisting of a sphere and a nanorod. Enlarged insets (a) and (b) show an illustration of the molecular arrangement of the charged (green) and neutral (white) lipid. Reprinted in part from ref. 1 with permission. Copyright 2008, American Chemical Society. Scale bar, 500nm.

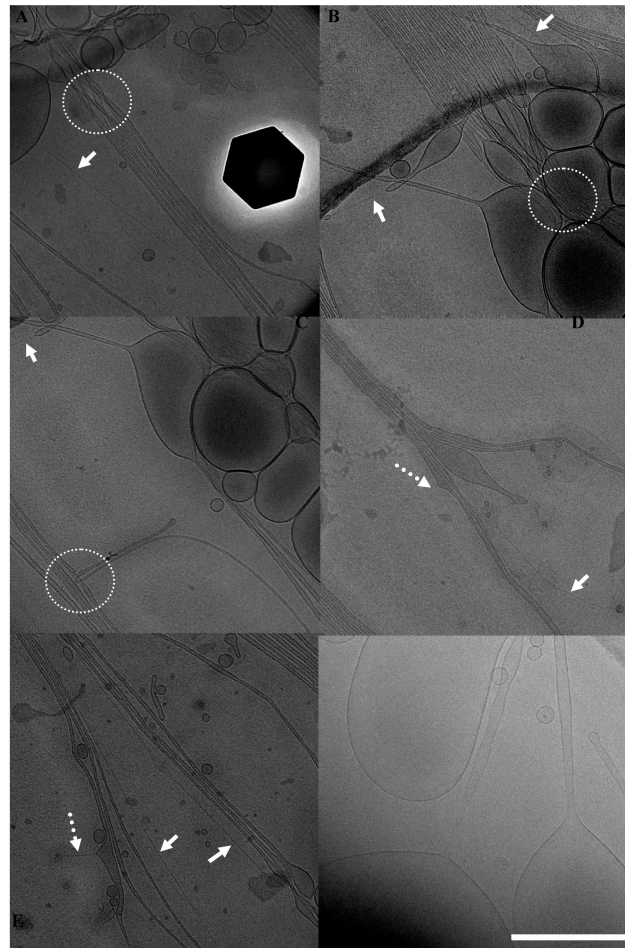


**Figure 3.**

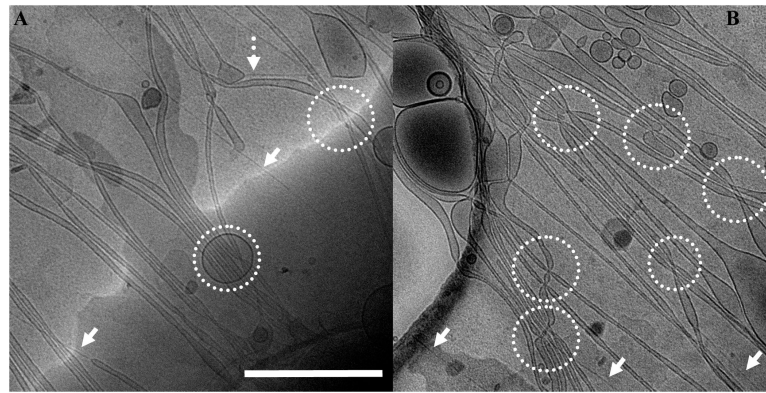
Cryo-TEM image of MVL3/DOPC BLs ( $\Phi_{MVL3}=0.1$ ). (A) This image is a collage of two separate sample views, thus expanding the observed area. The grey vertical line corresponds to the image boundary. White solid arrows point to the pearlizing instability occurring in this system. (B) A schematic drawing of a BL consisting of two spheres and a nanotube. Enlarged insets (a) and (b) show an illustration of the molecular arrangement of the charged (green) and neutral (white) lipid. Reprinted in part from ref. 1 with permission. Copyright 2008, American Chemical Society. Scale bar, 500 nm.

**Figure 4.**

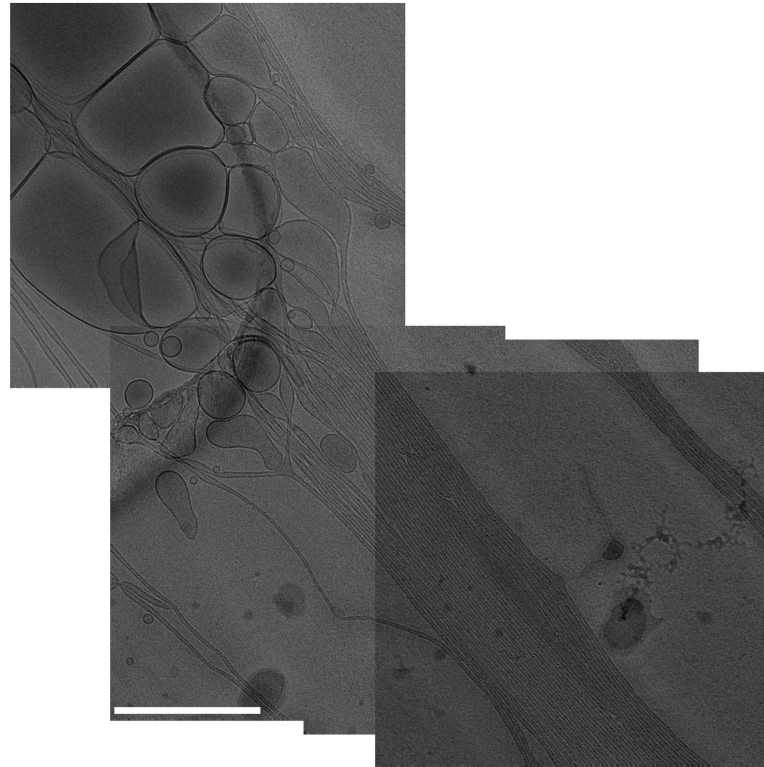
Low magnification cryo-TEM image of MVL5/DOPC BLs ( $\Phi_{MVL5}=0.1$ ). This lipid mixture forms an abundance of long nanotubes and BLs. The length of the nanotubes can be well over 10  $\mu\text{m}$ . The large circles in the image correspond to the holes in the carbon film on the copper grid. Scale bar, 2  $\mu\text{m}$ .

**Figure 5.**

Cryo-TEM images providing an overview of the most frequently observed features of MVL5/DOPC BLs ( $\Phi_{MVL5}=0.1$ ). White dotted circles highlight the areas where nanotubes are entangled. White solid arrows point to nanorods. Note the sphere–rod BL in panel A. White dotted arrows point to a unique feature of this system: “spikes”, which are nanorods budding off from a nanotube. Pronounced bundling of nanotubes is observed in panels A-E. Scale bar, 500 nm.

**Figure 6.**

Cryo-TEM images of MVL5/DOPC BLs ( $\Phi_{MVL5}=0.1$ ). Pronounced bundling can be observed. White dotted circles highlight areas where nanotubes cross or an entanglement of the nanotubes occurs at quite large length scales. White solid arrows point to nanorods. Scale bar, 500 nm.

**Figure 7.**

Superimposition of several cryo-TEM images of a large MVL5/DOPC nanotube bundle ( $\Phi_{MVL5}=0.1$ ). The bundling is maintained over more than 5  $\mu\text{m}$ . See Fig. S5 in the Supporting Information for a further expanded view with one additional image. Scale bar, 500 nm.